Renormalization algorithm for the calculation of spectra of interacting quantum systems

D. Porras,[1] F. Verstraete,[1,2] and J. I. Cirac[1]
[1]*Max-Planck Institut für Quantenoptik, Hans-Kopfermann-Str. 1, Garching D-85748, Germany*
[2]*Institute for Quantum Information, Caltech, Pasadena, California 91125, USA*
(Received 25 October 2005; published 13 January 2006)

We present an algorithm for the calculation of eigenstates with definite linear momentum in quantum lattices. Our method is related to the density matrix renormalization group, and makes use of the distribution of multipartite entanglement to build variational wave functions with translational symmetry. The algorithm is applied to the study of bilinear-biquadratic $S=1$ chains, in particular to the region of phase space between the dimerized and ferromagnetic phases.

DOI: 10.1103/PhysRevB.73.014410 PACS number(s): 75.10.Pq, 03.67.−a, 75.40.Mg

I. INTRODUCTION

Quantum many-body systems pose problems of great complexity that only in a few cases can be solved analytically. For this reason numerical algorithms have played a decisive role in understanding the rich phenomenology of strongly correlated matter. A remarkable example is the density matrix renormalization group (DMRG), which is recognized as a powerful tool for the description of ground state properties.[1] On the other hand, the recent merging of quantum information theory[2] and condensed matter has given us a unique insight into the physics of interacting quantum systems. The theory of entanglement has yielded tools to quantify quantum correlation,[3] as well as a theoretical framework for the understanding of the DMRG,[4] and the development of algorithms to deal with problems in higher dimensions,[5] and also to describe time evolution, systems at finite temperature and quantum dissipation.[6,7]

DMRG is a variational method over the class of matrix product states,[4,8] which correspond to the one-dimensional (1D) realization of the more general projected entangled pair states (PEPS) introduced in Ref. 5. In a PEPS each site in a lattice is described by a set of auxiliary systems which form entangled pairs with their neighbors, and the physical state is built by local projections in the physical Hilbert space. The distribution of bipartite entanglement governs the characteristics of PEPS, which are ideally suited to describe systems with short range correlations, something that explains why the DMRG is particularly accurate in describing noncritical ground states. This observation invites us to consider the intriguing possibility of modifying the auxiliary state underlying PEPS to distribute multipartite entanglement and build variational classes that are more suitable for a given problem.

This paper is structured as follows: In Sec. II we define the projected entangled multipartite states (PEMS) and study, as a particular realization, the case in which a GHZ like state is added to the auxiliary system underlying PEPS. The resulting variational states have a given definite linear momentum k. We show, in Sec. III how to use this variational class to describe efficiently excitations of translational invariant Hamiltonians by means of a numerical DMRG like algorithm. In this way, we can calculate the lowest energy branch of excitations, that is, the set of minimum energy eigenstates for different linear momenta $\{|\Psi_k^{[0]}\rangle\}$. In Sec. IV we present an algorithm for the calculation of the sequence of excited states at a given point in momentum space, $\{|\Psi_k^{[0]}\rangle, |\Psi_k^{[1]}\rangle, \ldots\}$, which has a broad usefulness, and can also be implemented together with nontranslational invariant DMRG related algorithms. In Sec. V, the utility of the method is shown in the study of bilinear-biquadratic $S=1$ spin chains, where we find indications of quantum critical phase characterized by nematic quasilong range order, which can be realized in experiments with cold atoms in optical lattices as shown in recent proposals.[9,10] Finally we present our conclusions.

II. PROJECTED ENTANGLED-MULTIPARTITE STATES

We introduce our method by considering the case of a chain of N d_s-dimensional spins. Let us assign a set of auxiliary subsystems x_n to each site n. In 1D PEPS, only adjacent sites are entangled in $|\Psi_{aux}\rangle$. To describe efficiently multipartite entanglement, such as the one present in critical or spin-wave-like states, one should consider the most general case in which $|\Psi_{aux}\rangle$ is multipartite entangled, that is, it cannot be reduced to a product state of pairs of entangled sites.[11] The physical wave function is created with the aid of a product of local projection operators, P_n

$$|\Psi_{PEMS}\rangle = P_1 \otimes P_2 \otimes \ldots \otimes P_N |\Psi_{aux}\rangle. \tag{1}$$

Each P_n describes a local mapping from x_n to the spin at site n. Let us see how the choice of the proper $|\Psi_{aux}\rangle$ allows us to find a variational class with translational invariance. Each site n is described with the aid of two auxiliary subsystems, a_n, b_n of dimension D and a third subsystem c_n of dimension N. a_n, b_{n+1} form a maximally entangled state, $|\phi\rangle$

$$|\phi\rangle := \sum_{\alpha=1}^{D} |\alpha\rangle|\alpha\rangle. \tag{2}$$

On the other hand, the c_n are in the following multipartite entangled state:[12]

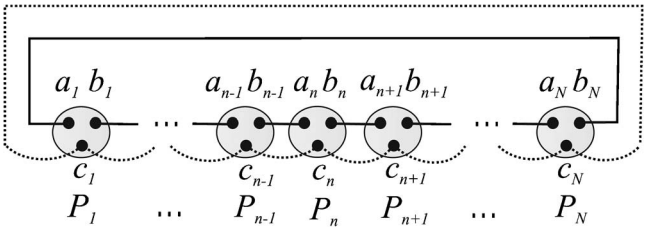

FIG. 1. Schematic picture of the projected entangled multipartite states presented in the text.

$$|M_k\rangle \equiv \frac{1}{\sqrt{N}} \sum_{n=0}^{N-1} e^{ikn} T_n |1\rangle_{c_1} |2\rangle_{c_2} \cdots |N\rangle_{c_N}, \tag{3}$$

where $k=n_k 2\pi/N$, with $n_k=0,\ldots,N-1$, and T_n is the operator that performs a translation of n sites. The auxiliary state is, thus, $|\Psi_{aux}\rangle=|\Phi\rangle^{\otimes N}|M_k\rangle$ (see Fig. 1).

In this case, contrary to the nontranslational ansatz in Ref. 4, all P_n's are given by the same operator acting on different sites of the chain, so that their product is a translational invariant operator. The local maps are determined by a set of Nd_s matrices of dimension D, $\{A^s_{[\gamma]}\}_{s=1,\ldots,d_s\,\gamma=1,\ldots,N}$,

$$P = \sum_{s,\alpha,\beta,\gamma} (A^s_{[\gamma]})_{\alpha,\beta} |s\rangle_a \langle\alpha|_b \langle\beta|_c \langle\gamma|, \tag{4}$$

such that P_n acts on the auxiliary states of site n and returns the spin state $|s\rangle$ with amplitude $(A^s_{[\gamma]})_{\alpha,\beta}$, provided a_n,b_n,c_n are in states $|\alpha\rangle,|\beta\rangle,|\gamma\rangle$, respectively. The resulting physical states form a variational class of translational invariant states with momentum k

$$|\Psi_k\rangle = \sum_{n=0,\{s_j\}}^{N-1} \frac{e^{ikn}}{\sqrt{N}} T_n \,\mathrm{tr}\{A^{s_1}_{[1]} A^{s_2}_{[2]} \cdots A^{s_N}_{[N]}\} |s_1\rangle \cdots |s_N\rangle. \tag{5}$$

The physical meaning of γ becomes clear in Eq. (5). Due to the presence of $|M_k\rangle$ the auxiliary state is projected in a linear combination of 1D PEPS formed by circular permutations of $A^s_{[\gamma]}$, in which γ represents the site in the chain. Note that (5) can be defined on lattices of any spatial dimension D_s, by considering first the D_s structure of PEPS presented in Ref. 5, and adding N^{D_s}-dimensional auxiliary subsystems $c_{\vec{n}}$, at each site $\vec{n}$. The auxiliary state $|M_{\vec{k}}\rangle$ is defined then by replacing k, n by D_s vectors in (3).

The class of states defined by Eq. (5) has a remarkable property: the maximum entropy of the reduced density matrix of a block of L sites is given by $S_L=\ln(ND^2)$, that is, it increases with the size of the system. On the contrary, in the nontranslational invariant ansatz,[4] the maximum entropy of a block follows the relation $S_L=\ln(D^2)$, that is, it is independent on N.

Averages of observables are computed efficiently with the aid of the following matrices of dimension D^2:

$$E^{n,d}_O = \sum_{s,s'} [A^s_{[n]} \otimes (A^{s'}_{[n-d]})^*] \langle s'|O|s\rangle, \tag{6}$$

with the following definition of tensor product:

$$(A \otimes B)_{(\alpha,\alpha'),(\beta,\beta')} = A_{\alpha,\beta} B_{\alpha',\beta'}. \tag{7}$$

From now on let us assume that (mod$N$) is implicit in functions of indexes n,m,d, which always run from 0 to $N-1$, such that periodic boundary conditions are satisfied. The expectation value of any operator turns out to be a linear combination of N products of $D^2\times D^2$ matrices

$$\langle O_1 O_2 \cdots O_N\rangle = \frac{1}{N} \sum_{n,d} e^{-ikd} \,\mathrm{tr}\{E^{n,d}_{O_1} E^{n+1,d}_{O_2} \cdots E^{n-1,d}_{O_N}\}. \tag{8}$$

Equation (8) shows that the calculation of averages is decomposed into a sum over N Fourier components.

III. MINIMIZATION OF THE ENERGY WITHIN THE PEMS VARIATIONAL CLASS

Let us see how to find the state of the form (5) that minimizes a given Hamiltonian. We consider for concreteness the case of a short range translational invariant spin model, $H=\Sigma_{\mu,n} g_\mu \sigma^\mu_n \sigma^\mu_{n+1}$, where σ^μ form an orthogonal set of Hermitian operators. The norm and the mean value of the energy can be calculated with the aid of Eq. (8)

$$\begin{aligned} \langle\Psi_k|\Psi_k\rangle &= \sum_d e^{-ikd} \,\mathrm{tr}\{E^{1,d}_1 \cdots E^{N,d}_1\}, \\ \langle\Psi_k|H|\Psi_k\rangle &= \sum_{d,\mu} g_\mu e^{-ikd} \,\mathrm{tr}\{E^{1,d}_{\sigma_\mu} E^{2,d}_{\sigma_\mu} \cdots E^{N,d}_1 + \cdots \\ &\quad + E^{1,d}_1 \cdots E^{N-1,d}_{\sigma_\mu} E^{N,d}_{\sigma_\mu}\}. \end{aligned} \tag{9}$$

Any expectation value calculated with (5) is a bilinear form of each $A^s_{[n]}$ separately, so that

$$\begin{aligned} \langle\Psi_k|\Psi_k\rangle &= A^\dagger_{[n]} \mathcal{N}[n] A_{[n]}, \\ \langle\Psi_k|H|\Psi_k\rangle &= A^\dagger_{[n]} \mathcal{H}[n] A_{[n]}, \end{aligned} \tag{10}$$

where $A_{[n]}$ is the vector obtained by contracting s, α, and β, in a single index. Thus, the energy can be minimized with respect to the set of matrices $A^s_{[n]}$ with a given n, by solving the generalized eigenvalue problem

$$\mathcal{H}[n] A_{[n]} = \epsilon_0 \mathcal{N}[n] A_{[n]}. \tag{11}$$

This fact allows us to find the optimum PEMS in an iterative way that is similar to other DMRG-like methods: once we have found the optimum $A^s_{[n]}$, we replace it in the wave function (5), something that defines a step in our algorithm. Then, we calculate $\mathcal{H}[n+1]$, $\mathcal{N}[n+1]$, and repeat the minimization with respect to $A^s_{[n+1]}$. We continue in the same vein along the whole chain, from $n=1$ to $n=N$, which defines a sweep. Several sweeps are performed until the energy converges, something that requires around 10 sweeps in the calculations presented below.

In the following we will explain how to calculate efficiently the bilinear forms in Eq. (10). According to Eq. (8), $\mathcal{H}[n]$ and $\mathcal{N}[n]$ can be expressed as a linear combination of Fourier components

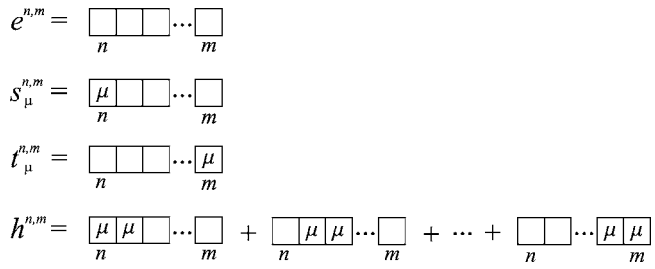

FIG. 2. Representation of the operators defined in Eqs. (14), which are used in the actualization of the effective Hamiltonian and norm operators. Empty and filled squares correspond to $E_1^{n,d}$ and $E_{\sigma^\mu}^{n,d}$, respectively.

$$\mathcal{N}[n] = \sum_d e^{-ikd}\mathcal{N}[n,d], \quad \mathcal{H}[n] = \sum_d e^{-ikd}\mathcal{H}[n,d], \quad (12)$$

where $\mathcal{N}[n,d]$, $\mathcal{H}[n,d]$ depend on matrices $E_O^{m,d}$, that is, on tensor products where one of the matrices $A_{[n]}^s$ is displaced in the index n a number d of sites, with respect to the other. In order to find an explicit expression for the bilinear forms (10), we notice first that matrices $A_{[n]}^s$ appear twice in each product in Eq. (8), both in $E_O^{n,d}$ and $E_O^{n+d,d}$. For example,

$$\begin{aligned}\mathcal{N}[n,d]_{\binom{s}{\alpha\beta},\binom{s'}{\alpha'\beta'}} &= \mathrm{tr}\left\{\left(\chi\begin{bmatrix}\alpha'\\ \beta'\end{bmatrix}\otimes (A_{[n-d]}^{s'})^*\right)E_1^{n+1,d}\cdots E_1^{n+d-1,d}\right.\\ &\left.\times\left(A_{[n+d]}^s\otimes\chi\begin{bmatrix}\alpha\\ \beta\end{bmatrix}\right)E_1^{n+d+1,d}\cdots E_1^{n-1,d}\right\}, \quad (13)\end{aligned}$$

where $\chi\left[\begin{smallmatrix}\alpha\\ \beta\end{smallmatrix}\right]$ is a $D\times D$ matrix with all elements 0, but a 1 in the entry (α,β). A similar expression can be found for

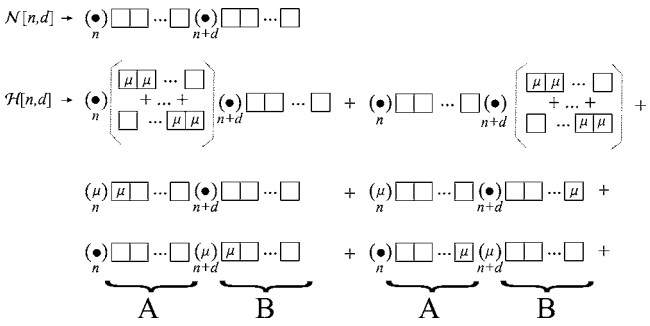

FIG. 3. Representation of Eqs. (15). Parentheses represent sites where matrices $A_{[n]}^s$ appear in (9). (•) corresponds to terms of the form $\chi\otimes(A_{[n]}^s)^*$ or $A_{[n]}^s\otimes\chi$, whereas (μ) corresponds to contractions with the operator σ^μ, that is, terms of the form: $\Sigma_s\chi\otimes(A_{[n]}^t)^*\sigma_{t,s}^\mu$ or $\Sigma_s(A_{[n]}^t)\sigma_{t,s}^\mu\otimes\chi$.

$\mathcal{H}[n,d]$, which includes a sum over N terms that correspond to each interaction in the Hamiltonian, and involves also products of $E_{\sigma_\mu}^{n,d}$. In order to put expressions like (13) in a more compact form, we introduce the following set of operators (Fig. 2)

$$\begin{aligned}e_d^{n,m} &= E_1^{n,d}E_1^{n+1,d}\cdots E_1^{m,d},\\ s_{\mu,d}^{n,m} &= E_{\sigma^\mu}^{n,d}E_1^{n+1,d}\cdots E_1^{m,d},\\ t_{\mu,d}^{n,m} &= E_1^{n,d}E_1^{n+1,d}\cdots E_{\sigma^\mu}^{m,d},\end{aligned} \quad (14)$$

$$h_d^{n,m} = \sum_\mu g_\mu(E_{\sigma^\mu}^{n,d}E_{\sigma^\mu}^{n+1,d}\cdots E_1^{m,d} + \cdots + E_1^{n,d}\cdots E_{\sigma^\mu}^{m-1,d}E_{\sigma^\mu}^{m,d}).$$

In terms of (14) we can rewrite Eq. (13), as well as the Hamiltonian Fourier components (see Fig. 3)

$$\begin{aligned}\mathcal{N}[n,d]_{\binom{s}{\alpha\beta},\binom{s'}{\alpha'\beta'}} &= \mathrm{tr}\left\{\left(\chi\begin{bmatrix}\alpha'\\ \beta'\end{bmatrix}\otimes (A_{[n-d]}^{s'})^*\right)e_d^{n+1,n+d-1}\left(A_{[n+d]}^s\otimes\chi\begin{bmatrix}\alpha\\ \beta\end{bmatrix}\right)e_d^{n+d+1,n-1}\right\},\\ \mathcal{H}[n,d]_{\binom{s}{\alpha\beta},\binom{s'}{\alpha'\beta'}} &= \mathrm{tr}\left\{\left(\chi\begin{bmatrix}\alpha'\\ \beta'\end{bmatrix}\otimes (A_{[n-d]}^{s'})^*\right)h_d^{n+1,n+d-1}\left(A_{[n+d]}^s\otimes\chi\begin{bmatrix}\alpha\\ \beta\end{bmatrix}\right)e_d^{n+d+1,n-1}\right\}\\ &+ \mathrm{tr}\left\{\left(\chi\begin{bmatrix}\alpha'\\ \beta'\end{bmatrix}\otimes (A_{[n-d]}^{s'})^*\right)e_d^{n+1,n+d-1}\left(A_{[n+d]}^s\otimes\chi\begin{bmatrix}\alpha\\ \beta\end{bmatrix}\right)h_d^{n+d+1,n-1}\right\}\\ &+ \sum_\mu g_\mu\,\mathrm{tr}\left\{\left(\chi\begin{bmatrix}\alpha'\\ \beta'\end{bmatrix}\otimes\sum_t (A_{[n-d]}^t)^*\sigma_{t,s'}^\mu\right)s_{\mu,d}^{n+1,n+d-1}\left(A_{[n+d]}^s\otimes\chi\begin{bmatrix}\alpha\\ \beta\end{bmatrix}\right)e_d^{n+d+1,n-1}\right\}\\ &+ \sum_\mu g_\mu\,\mathrm{tr}\left\{\left(\chi\begin{bmatrix}\alpha'\\ \beta'\end{bmatrix}\otimes\sum_t (A_{[n-d]}^t)^*\sigma_{t,s'}^\mu\right)e_d^{n+1,n+d-1}\left(A_{[n+d]}^s\otimes\chi\begin{bmatrix}\alpha\\ \beta\end{bmatrix}\right)t_{\mu,d}^{n+d+1,n-1}\right\}\\ &+ \sum_\mu g_\mu\,\mathrm{tr}\left\{\left(\chi\begin{bmatrix}\alpha'\\ \beta'\end{bmatrix}\otimes (A_{[n-d]}^{s'})^*\right)e_d^{n+1,n+d-1}\left(\sum_t A_{[n+d]}^t\sigma_{t,s}^\mu\otimes\chi\begin{bmatrix}\alpha\\ \beta\end{bmatrix}\right)s_{\mu,d}^{n+d+1,n-1}\right\}\\ &+ \sum_\mu g_\mu\,\mathrm{tr}\left\{\left(\chi\begin{bmatrix}\alpha'\\ \beta'\end{bmatrix}\otimes (A_{[n-d]}^{s'})^*\right)t_{\mu,d}^{n+1,n+d-1}\left(\sum_t A_{[n+d]}^s\sigma_{t,s}^\mu\otimes\chi\begin{bmatrix}\alpha\\ \beta\end{bmatrix}\right)e_d^{n+d+1,n-1}\right\}.\end{aligned} \quad (15)$$

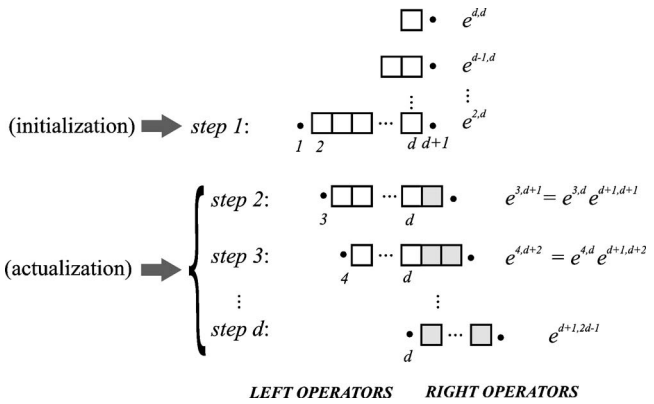

FIG. 4. Representation of the procedure for initialization and actualization of operators in the calculation of $e^{n+1,n+d-1}$. Empty and gray squares are left and right operators, respectively, as defined in the text.

In principle Eqs. (15) allow us to calculate directly $\mathcal{H}[n,d]$, and $\mathcal{N}[n,d]$, at each step. This would imply to multiply N^3 times E_O matrices (corresponding to N sites, N interacting terms in the Hamiltonian, and N values of d). Since the calculation of $\mathcal{H}[n,d]$, and $\mathcal{N}[n,d]$, is the most time demanding part of our algorithm, it is important to find a way to reduce this number of operations. Indeed, the number of multiplications can be reduced to scale like N by storing and actualizing products of matrices in a way that resembles the procedure for building block operators in the DMRG. Let us see how this procedure works.

In order to calculate $\mathcal{H}[n,d]$, and $\mathcal{N}[n,d]$, we have to compute the operators defined by the set of products (14). These ones can be calculated efficiently by using results of the previous steps, and recursive relations between operators. We notice that one has to perform this calculation independently for each Fourier component d. Furthermore, we need two sets of operators: each of them corresponds to series of products of E_O matrices that start at sites n, and $n+d$, respectively. In the following we will borrow the DMRG terminology and refer to these two sets as blocks A and B, as depicted in Fig. 3. The procedure that we explain below has to be carried out independently for each of the two blocks A, B.

Let us consider the case of the operators $e_d^{n+1,n+d-1}$, $s_{\mu,d}^{n+1,n+d-1}$, $t_{\mu,d}^{n+1,n+d-1}$, $h_d^{n+1,n+d-1}$, which appear in the block A of (15). In the first step, that is, $n=1$, we have to calculate and store a set of "left operators," $e_d^{n',d}$, $s_{\mu,d}^{n',d}$, $t_{\mu,d}^{n',d}$, and $h_d^{n',d}$, with $n'=2,\ldots,d$. The initialization of the left operators can be done efficiently by means of the following recursive relations:

$$e_d^{n',d} = E_1^{n',d} e_d^{n'-1,d},$$

$$s_{\mu,d}^{n',d} = E_{\sigma^\mu}^{n',d} e_d^{n'-1,d},$$

$$t_{\mu,d}^{n',d} = E_1^{n',d} t_d^{n'-1,d},$$

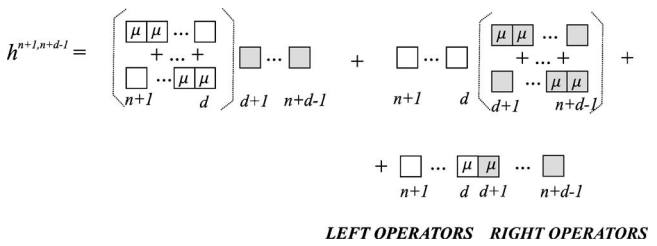

FIG. 5. Actualization of the operator $h^{n+1,n+d-1}$ by using left and right operators.

$$h_d^{n',d} = \sum_\mu g_\mu E_{\sigma^\mu}^{n',d} s_{\mu,d}^{n'-1,d} + E_1^{n',d} h_d^{n'-1,d}. \tag{16}$$

In Fig. 4 we represent this part of the algorithm in the case of $e^{n',d}$. After solving the eigenvalue problem for $A_{[1]}^s$, we move to the following sites, $n=2,\ldots,1-d$. In the following steps we actualize (but do not need to store), "right operators" at each step n: $e_d^{d+1,n+d-1}$, $s^{d+1,n+d-1}$, $t_{\mu,d}^{d+1,n+d-1}$, $h^{d+1,n+d-1}$, by using the right operators of the previous step $n-1$, and the recursion relations equivalent to (16). At each step left and right operators are combined to calculate the matrices that we need for (15). For example (see Fig. 5)

$$h_d^{n+1,n+d-1} = h_d^{n+1,d} e_d^{d+1,n+d-1} + e_d^{n+1,d} h_d^{d+1,n+d-1} + \sum_\mu g_\mu t_{\mu,d}^{n+1,d} s_{\mu,d}^{d+1,n+d-1}. \tag{17}$$

This procedure for initialization and actualization of operators is carried out independently at each step in the calculation of each Fourier component $\mathcal{H}[n,d]$, $\mathcal{N}[n,d]$, such that the number of matrix multiplications necessary for a step corresponding to finding the optimal value of a matrix $A_{[n]}^s$, scales like N, because of the N Fourier components. To perform a sweep along the chain we need N steps, and thus, the whole algorithm scales like N^2.

IV. CALCULATION OF THE SET OF EXCITED STATES WITH A GIVEN LINEAR MOMENTUM

In the following we show how to modify our method to obtain the sequence of excited states with a given linear momentum. Let us consider that we have previously calculated the M lowest energy eigenstates, $|\Psi_k^{[j]}\rangle$, with linear momentum k, described by the set of matrices $B[j]_{[\gamma]}^s$. In order to proceed further and find the $M+1$ lowest energy state, we would like to run the optimization algorithm under the following constraint:

$$\langle \Psi_k^{[j]} | \Psi_k \rangle = 0, \quad \forall\, j = 1, \ldots, M. \tag{18}$$

Within the variational class of 1D PEMS defined by (5), each constraint in Eq. (18) is given by

$$\langle \Psi_k^{[j]} | \Psi_k \rangle = \sum_{d=0}^{N-1} e^{-ikd} \operatorname{tr}\{E_{[j]}^{1,d} E_{[j]}^{2,d} \cdots E_{[j]}^{N,d}\}, \tag{19}$$

where we use the definition

$$E^{n,d}_{[j]} = \sum_s A^s_{[n]} \otimes (B[j]^s_{[n-d]})^*. \quad (20)$$

Equation (18) implies a linear constraint in the optimization with respect to each $A^s_{[n]}$ separately. In order to include this constraint in our algorithm we proceed as follows. At each step n we use (20) to calculate the linear form $\mathcal{B}[j,n]$ that imposes the orthogonality to $|\Psi^{[j]}_k\rangle$ in terms of $A^s_{[n]}$

$$\langle \Psi^{[j]}_k | \Psi_k \rangle = \sum_{s,\alpha,\beta} ((\mathcal{B}[j,n])^s_{\alpha,\beta})^* (A^s_{[n]})_{\alpha,\beta} = 0. \quad (21)$$

$\mathcal{B}[j,n]$ can also be decomposed into Fourier components, in the same way as $\mathcal{H}[n]$, $\mathcal{N}[n]$:

$$\mathcal{B}[j,n] = \sum_d e^{-ikd} \mathcal{B}[j,n,d]. \quad (22)$$

Each of these components can be computed by the same procedure for actualization and storage of blocks that was explained below. If we contract (s,α,β) in a single index, then (21) reads: $B[j,n]^\dagger A_{[n]}=0$. The linear constraint is incorporated to the optimization procedure by defining projectors in the subset of states that are orthogonal to the M lowest states, that is

$$\mathcal{P}[n] = 1 - \sum_{i,j} B[i,n](N_B^{-1})_{i,j} B[j,n]^\dagger, \quad (23)$$

with $(N_B)_{i,j}=B[i,n]^\dagger B[j,n]$. The eigenvalue problem is now defined by the new Hamiltonian and norm matrices given by

$$\mathcal{H}[n] \to \mathcal{P}[n]\mathcal{H}[n]\mathcal{P}[n], \quad \mathcal{N}[n] \to \mathcal{P}[n]\mathcal{N}[n]\mathcal{P}[n]. \quad (24)$$

The same idea can be used in other DMRG related algorithms, because orthogonality to a set of lower energy states can always be expressed as a linear constraint at each step in the optimization. In this way, low-energy excitations can be calculated in a controlled way as an optimization procedure.

V. APPLICATION TO THE BILINEAR-BIQUADRATIC $S=1$ SPIN CHAIN

We have applied our method to the study of the bilinear-biquadratic $S=1$ chain

$$H = \sum_i h_{i,i+1} = \sum_i \cos(\theta)\vec{S}_i\vec{S}_{i+1} + \sin(\theta)(\vec{S}_i\vec{S}_{i+1})^2. \quad (25)$$

This model displays a rich variety of phases depending on the parameter θ, and its realization in experiments with optical lattices has been recently proposed.[9,10] We focus here on the region $-3\pi/4 \leqslant \theta \leqslant -\pi/2$, whose characteristics have been yet not fully understood. The two limits, $-\pi/2$, $-3\pi/4$, are exactly solvable and correspond to a gapped dimerized,[13] and a gapless ferromagnetic phase,[14] respectively. So far, it has remained unclear what happens between the dimerized and ferromagnetic phases, in particular, whether the dimer order survives down to $\theta=-3\pi/4$. In Ref. 15, it was conjectured that a 1D quantum nematic phase should appear as an intermediate phase. Since then, a few numerical works have dealt with this problem,[16–19] but this phase is yet not fully characterized.

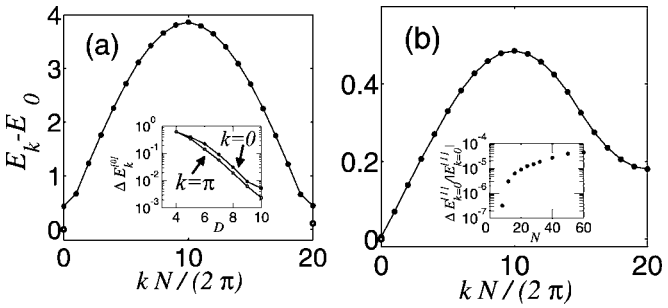

FIG. 6. Lowest states of a bilinear-biquadratic $S=1$ chain, $N=40$ sites, $D=10$. (a) $\theta=-\pi/2$, $E_0=-2.7976N$, (b) $\theta=-0.74\pi$, $E_0=-1.4673N$. Empty circles: lowest energy states. Filled circles: first branch of excitations. Estimated absolute error $\Delta E_k \approx 5\times 10^{-3}$. Inset (a): error in the absolute energies $E_0^{[0]}$, $E_\pi^{[0]}$ as a function of D, estimated by comparison with $D=14$ calculations, for $\theta=-0.5\pi$. The convergence of the algorithm has also been checked with other values of k, yielding similar results. Inset (b): relative error as a function of N in the first excited state energy with $k=0$, $\theta=-\pi/2$.

The ability to calculate excitations in a controlled way, makes our algorithm ideally suited to deal with this problem. Figure 6 shows the spectrum of low energy states at two different points in the phase diagram. At $\theta=-\pi/2$ the dispersion relation corresponds qualitatively to a gapped phase. Note that for the calculation of the spectrum it is necessary to include the constraint (18), in order to find the second lowest energy state at points $k=0$, $k=\pi$. At $\theta=-0.74\pi$, which lies within the conjectured quantum nematic phase, the spectrum shows a qualitative change that involves the appearance of a soft mode. The convergence of the algorithm with D is shown in Fig. 6(a). At $\theta=-\pi/2$ we compare our results for the excited state $E^{[1]}_{k=0}$ with exact results obtained by Bethe ansatz.[13] The absolute error in the ground state, calculated by the extrapolation of $E_0^{[0]}$ to $D=12$ ($\Delta E_0^{[0]}=2\times 10^{-3}$) agrees with the error in the first excited state ($\Delta E_0^{[1]}=3\times 10^{-3}$) obtained from the comparison with the exact result at $\theta=-\pi/2$. We have also checked that our algorithm converges with D for other values of the linear momentum k, such that it describes well the whole spectrum of low-energy excitations.

By means of Eq. (8) we can also calculate order parameters (OP) in the ground state. Long range dimer order is characterized by a nonzero value of $\langle \mathcal{D}^2 \rangle / N^2$ in the thermodynamical limit, where

$$\mathcal{D} = \sum_i (-1)^i h_{i,i+1}, \quad (26)$$

is the bond-strength oscillation. In the interval $\theta \leqslant \theta_c$, $\theta_c \approx -0.7\pi$, our finite size results are extrapolated to a value $\mathcal{D}^2/N^2 < 3\times 10^{-5}$, which is set by our accuracy, estimated by comparison with higher D calculations [Fig. 7(a)]. On the other hand the nematic OP is given by the quadrupole tensor, whose components are rotations of

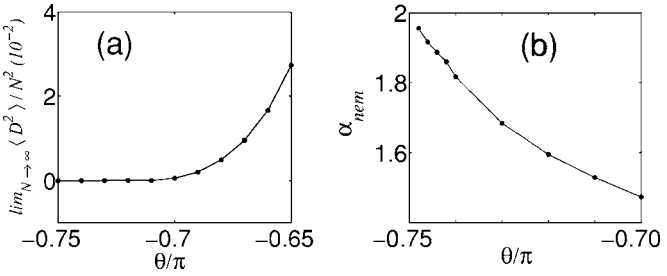

FIG. 7. (a) Extrapolated dimer order parameter. (b) Exponent of the squared quantum nematic order parameter. In both cases $8 < N < 36$, and $D=12$ ($D=14$ for $N>28$).

$$\mathcal{Q}^{zz} = \sum_i [(S_i^z)^2 - 2/3]. \tag{27}$$

Long-range nematic order is described by the isotropic squared OP

$$\mathcal{Q}^2 = \int d\Omega \langle (\mathcal{Q}_\Omega^{zz})^2 \rangle, \tag{28}$$

where $\mathcal{Q}_\Omega^{zz}$ is $\mathcal{Q}^{zz}$ rotated to the solid angle Ω. We find that $\mathcal{Q}^2(N) \propto N^{\alpha_{nem}}$ in the interval $-3\pi/4 < \theta < \theta_c$ with $1.4 < \alpha_{nem} < 2$ [see Fig. 7(b)]. Thus, long-range nematic order is absent, in qualitative agreement with Coleman's theorem.[20] The fact that $\mathcal{Q}^2$ decays algebraically with $\alpha_{nem} > 1$ is consistent with the existence of quasi-long-range order, as defined by algebraic decay of nematic correlation functions.[21] Note that α_{nem} evolves continuously to the value $\alpha_{nem}=2$ in agreement with the exact solution at $\theta=-3\pi/4$.[14]

The spectrum in the thermodynamical limit can be accurately determined by studying the scaling of the gaps with system size. In particular, the gap between $k=0$, and $k=\pi$ is extrapolated to zero within our numerical accuracy ($\Delta E < 10^{-3}$) in the whole region under study [Fig. 8(a)]. We have also studied the scaled gap between the lowest $k=0$ states, $N(E_0^{[1]} - E_0^{[0]})$. This quantity should grow linearly with N in a gapped phase; however, for values $\theta \leqslant \theta_c$ the $k=0$ the scaled gap saturates [Fig. 8(b)]. Our results in the range $\theta \leqslant \theta_c$, $\theta_c \approx -0.7\pi$ are thus consistent either with (i) a gapless quantum phase with nematic quasilong range order, (ii) a phase with correlation lengths longer than the size of the chains considered here, in which case Fig. 8 would not correspond to the asymptotic regime, or (iii) a gap that is smaller than our numerical accuracy.

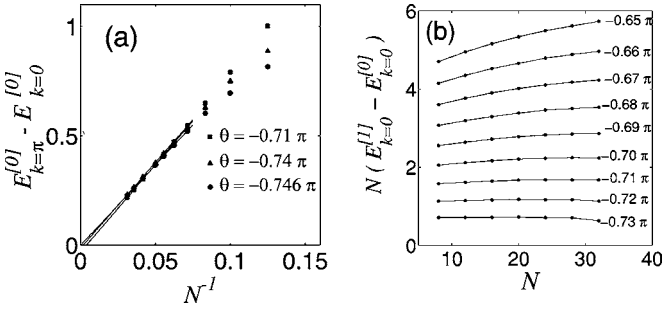

FIG. 8. (a) Finite size scaling of the gap between the lowest $k=0$, and $k=\pi$ states. The lines are the extrapolation to $N \to \infty$. (b) Scaled gap between the lowest energy $k=0$ states. In both plots $D=12$ ($D=14$, for $N=32$), and the error in E_k is $=10^{-3}$.

VI. CONCLUSIONS

We have presented a DMRG-like variational algorithm that allows us to find the lowest energy states with a definite momentum of translational invariant Hamiltonians. The variational class of states we used in the algorithms was obtained by extending the concept of projected entangled pair states to include a particular multipartite entangled state. An interesting extension of this work is to explore how other multipartite states with long-range correlations could help in simulating, e.g., critical systems.

ACKNOWLEDGMENTS

We thank M. A. Martín Delgado, G. Ortiz, E. Demler, E. Altmann, and S. Montangero, for interesting discussions. The work was supported by DFG (SFB 631), European projects, Bayerischen Staatsregierung Quanteninformation, MEIF-CT-2004-010350, and the Gordon and Betty Moore Foundation (the Information Science and Technology Initiative, Caltech).

[1] S. R. White, Phys. Rev. Lett. **69**, 2863 (1992); Phys. Rev. B **48**, 10345 (1992).

[2] M. Nielsen and I. Chuang, *Quantum Computation and Quantum Information* (Cambridge University Press, Cambridge, 2000).

[3] G. Vidal, J. I. Latorre, E. Rico, and A. Kitaev, Phys. Rev. Lett. **90**, 227902 (2003).

[4] F. Verstraete, D. Porras, and J. I. Cirac, Phys. Rev. Lett. **93**, 227205 (2004).

[5] F. Verstraete and J. I. Cirac, cond-mat/0407066 (unpublished).

[6] F. Verstraete, J. J. García-Ripoll, and J. I. Cirac, Phys. Rev. Lett. **93**, 207204 (2004).

[7] G. Vidal, Phys. Rev. Lett. **93**, 040502 (2004).

[8] S. Ostlund and S. Rommer, Phys. Rev. Lett. **75**, 3537 (1995).

[9] J. J. García-Ripoll, M. A. Martín-Delgado, and J. I. Cirac, Phys. Rev. Lett. **93**, 250405 (2004).

[10] A. Imambekov, M. Lukin, and E. Demler, Phys. Rev. A **68**, 063602 (2003).

[11] For example, $|\Psi_{aux}\rangle$ can be the critical ground state of an exactly solvable model, such that local variables in the $|\Psi_{PEMS}\rangle$ are long range correlated.

[12] $|M\rangle_k$ is equivalent to the multipartite GHZ state, $(1/\sqrt{N})(|1\cdots1\rangle + |2\cdots2\rangle + \cdots |N\cdots N\rangle)$, up to local unitary operations.

[13] M. N. Barber and M. T. Batchelor, Phys. Rev. B **40**, 4621 (1989); A. Klümper, J. Phys. A **23**, 809 (1990).

[14] C. D. Batista, G. Ortiz, and J. E. Gubernatis, Phys. Rev. B **65**, 180402 (2002).

[15] A. V. Chubukov, Phys. Rev. B **43**, 3337 (1991).
[16] G. Fáth and J. Sólyom, Phys. Rev. B **51**, 3620 (1995).
[17] A. Läuchli, G. Schmid, and S. Trebst, cond-mat/0311082 (unpublished); M. Rizzi, D. Rossini, G. De Chiara, S. Montangero, and Rosario Fazio, Phys. Rev. Lett. **95**, 240404 (2005).
[18] N. Kawashima, Prog. Theor. Phys. **145**, 138 (2002).
[19] K. Buchta, G. Fáth, Ö. Legeza, and J. Sólyom, Phys. Rev. B **72**, 054433 (2005).
[20] S. Colemann, Chem. Phys. **31**, 259 (1973).
[21] A. Auerbach, *Interacting Electrons and Quantum Magnetism* (Springer-Verlag, New York, 1994).